Generation of Spiral Shape Nitrogen Recombining Plasma for Atomic Nitrogen Source*)

Koji ASAOKA, Noriyasu OHNO, Yuki HAYASHI[1)], Shin KAJITA[2)] and Hirohiko TANAKA

Graduate School of Engineering, Nagoya University, Nagoya 466-8603, Japan

[1)]*National Institute for Fusion Science, National Institutes of Natural Sciences, Toki 509-5292, Japan*

[2)]*Institute of Materials and Systems for Sustainability, Nagoya University, Nagoya 466-8603, Japan*

(Received 9 January 2019 / Accepted 27 February 2019)

We propose a new method using a spiral shape nitrogen plasma with a long magnetic connection length to produce high density nitrogen (N) atoms for nitriding application. A high density N molecular ion plasma was generated by DC discharge and is transported along a long spiral magnetic field line. As a result, the electron temperature drops along the magnetic field to be low enough to produce dissociate recombining plasma, where dissociative recombination would occur to generate N atoms. 2D Langmuir probe measurement showed that the electron temperature and density decreased along the magnetic field. Optical emission spectroscopy showed the ratio of the atomic N and N molecular emission intensities increased with a discharge power. The ground state N atom density was estimated by analyzing the atomic line intensity.

Keywords: nitrogen atom source, dissociative recombination, spiral shape plasma, nitriding method, NAGDIS-T

DOI: 10.1585/pfr.14.3401069

1. Introduction

It is commonly known that nitriding metal can improve abrasion, fatigue, corrosion, and heat resistance. Because it could make the lifetime of materials longer, various nitriding methods have been actively studied. One of the methods is gas nitriding with ammonia. However, this method requires to heat up materials over 50 hours and produces fragile compound layer on the surface [1]. Another method is ion nitriding, which is carried out in a nitrogen-hydrogen gas mixture at several Torr pressure. A glow discharge is operated with the sample as the cathode to be hardened [2]. This method also has several disadvantages: materials are damaged by ions accelerated by the electric field and the surface treatment area depends on plasma size.

In order to overcome the disadvantages mentioned above, the radical nitriding method was proposed. In this method, the materials are irradiated with nitrogen atom (N) radicals to form a nitrided surface without damage by ion bombardment. The most important task in this method is to produce high density N atoms. However, with conventional plasma discharges, it is difficult to generate high density N atoms because dissociation of N molecule by electron impact collision hardly occurs due to the high binding energy of the N molecule at 8.80 eV [3].

The electron-beam-excited plasma (EBEP) source has been developed to generate the N atoms with the dissociation process of N molecules induced by high energetic electron beam, and the generated atomic N density is of the order of 10^{17} m^{-3} [4]. After 6.5 hours treatment by this method, The nitride layer of 100 μm was obtained and the hardness of the surface reached 1000 HV(0.1) [5]. Figure 1 shows the rate coefficient of ionization and dissociative recombination between 0.01 and 100 eV. The rate coefficient of ionization was calculated from the cross-section data reported by Halas *et al.* [6]. Peterson *et al.* reported that the rate coefficient of dissociative recombination data were well fitted between 0.01 and 0.1 eV with the formula; $\langle\sigma v\rangle = 1.70 \times 10^{-13}\,(eT_e/300k_B)^{-0.30}$ [m^3 s^{-1}], where e is the elementary charge and k_B is the Boltzmann constant [7]. The EBEP method aims to generate the N atoms by electron impact dissociation ($N_2 + e^- \rightarrow N + N^+ + 2e^-$). However, the figure indicates that molecular N ions are dominant ion species in the conventional discharge with an

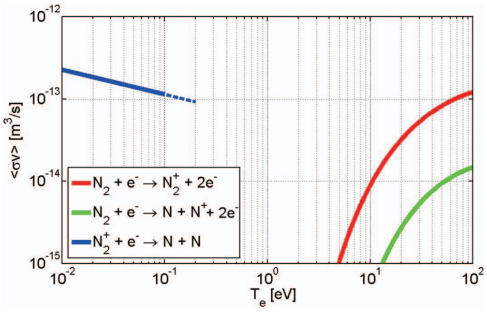

Fig. 1 Rate coefficient of electron impact ionization and dissociative recombination processes.

author's e-mail: asaoka.koji@f.mbox.nagoya-u.ac.jp

*) This article is based on the presentation at the 27th International Toki Conference (ITC27) & the 13th Asia Pacific Plasma Theory Conference (APPTC2018).

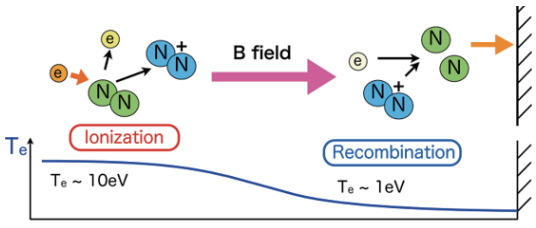

Fig. 2 Schematic of our proposed method to produce high density nitrogen atom.

electron temperature less than 10 eV due to the ionization process ($N_2 + e^- \rightarrow N_2^+ + 2e^-$).

On the other hand, when the electron temperature is decreased to be less than 1 eV, the rate coefficient for the dissociative recombination of the molecular N ions ($N_2^+ + e^- \rightarrow N + N$) becomes significantly large to produce N atoms from molecular N ions. Based on this process, the alternative method, an expanding supersonic nitrogen arc-jet plasma has been extensively researched for understanding about the reentry of a shuttle into the Earth's atmosphere and for applications of engineering, such as the polymerization and the metal surface modification [8–10]. In the arc-jet plasma, N molecules are highly ionized and flow to expansion region. Because of the diameter of the chamber is much larger than the diameter of the nozzle electrode, electrons with residual gas molecules in the expanding region are rapidly cooled. In this process, dissociative recombination occurs and N atoms are generated. The expanding nitrogen arc-jet method is expected to become high density atomic N source and creates a high quality nitride layer on the surface of the material with economic excellence. Akatsuka *et al.* reported the generated N atom density is 10^{24} m^{-3} maximum at the arc discharge region. The loss of nitrogen atoms to the wall is small because of supersonic arc-jet [11]. Ichiki *et al.* reported about a new nitriding method in which pulsed-arc plasma jet with N and hydrogen mixture gas is used. This method can be used in the atmospheric pressure. Further, materials are not biased, contributing to the low ion damage on the material surfaces. However, in this method, thin oxide layer is formed because of residual oxygen and it interrupts nitriding. In addition, the surface treatment area depends on the pulsed-arc plasma size [12].

In this paper, we propose an alternative new method to generate a higher density atomic N source based on dissociate recombining process. Figure 2 shows the schematic of our proposed method to produce high-density nitrogen atom. First, a high density and large size plasma in which molecular N ions are dominating is generated in the upstream region by utilizing DC discharge. Next, the produced high density and large size plasma is transported along the long magnetic field and cooled down to ~1 eV. As a result, the plasma condition is changed from ionizing to recombining phase, where dissociative recombination would occur to generate high density N atoms. It is expected that high-density N atoms could realize a faster nitriding process without the ion injection damages. Further, a high-quality diffusion layer which has large surface area thickness uniformity is expected to be formed on the surface without forming the compound layer.

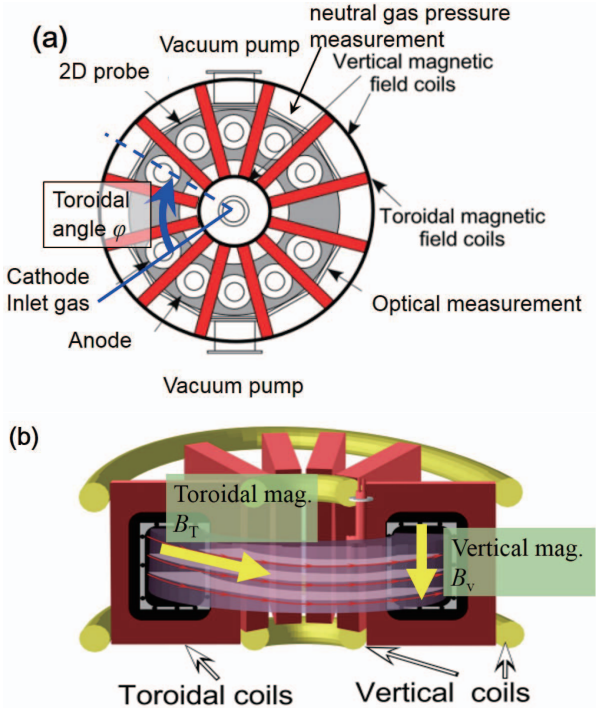

Fig. 3 (a) The top view of the NAGDIS-T. (b) The schematic diagram of NAGDIS-T with two types of the magnetic fields.

It is an important issue how to generate high density N plasma with long magnetic connection length with a relatively small apparatus size.

2. Experimental Setup

Figure 3 (a) shows a top view of NAGDIS-T (**Nag**oya University **Di**vertor **S**imulator with **T**oroidal magnetic configuration) [13]. A toroidal angle (φ) is defined as the angle from the cathode in the clockwise direction. The major radius is 340 mm and poloidal cross-section is 280 × 180 mm^2. This device has two magnetic fields, toroidal magnetic field (B_T) and vertical magnetic field (B_v), as shown in Fig. 3 (b). The maximum B_T was 0.10 T and the maximum B_v was 3.0×10^{-3} T. By using the two magnetic field, we can generate spiral shape magnetic field with the long connection length (L_C) between the top and bottom walls.

Figure 4 (a) show a picture of the plasma production region. The cathode was located at the bottom of the vacuum vessel. A circular-shape lanthanum hexaboride (LaB_6) with a diameter of 108 mm, which was heated by a carbon heater. The anode was a rectangle plate made

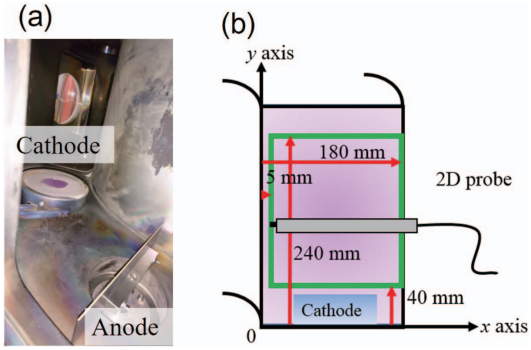

Fig. 4 (a) The NAGDIS-T DC discharge system. (b) The schematic diagram of the 2D Langmuir probe measurement.

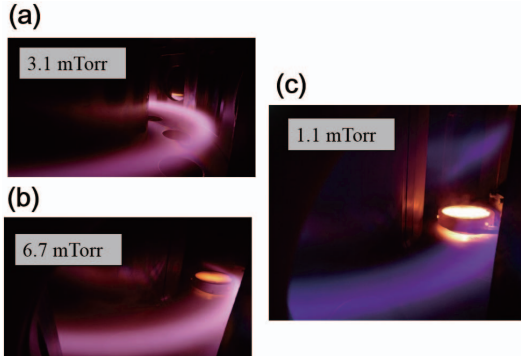

Fig. 5 Pictures of spiral shape plasmas at (a) p_n = 3.1 mTorr, I_d = 10 A, V_d = 130 V, (b) p_n = 6.7 mTorr, I_d = 10 A, V_d = 60 V, and (c) p_n = 1.1 mTorr, I_d = 1 A, V_d = 190 V.

of tungsten. The width was 170 mm, and the height was 35 mm.

A 2D Langmuir probe was installed at $\varphi = 90°$. 2D distribution of ion saturation current I_{sat} was obtained inside the green square region, shown in Fig. 4 (b). The electron temperature, T_e, and density, n_e, were also evaluated by single probe method.

A 0.75-m Czerny-Turner spectrograph (f = 750 mm) with a 1800 grooves/mm grating was used at $\varphi = 240°$. The measurement resolution was 0.013 nm, and the slit width was 50 μm.

3. Experimental Results

3.1 2D distribution of ion saturation current at various discharge conditions

Figures 5 (a - c) show pictures of the plasmas at B_T = 8.3 mT and B_v = 0.60 mT taken at $\varphi = 60°$ with different gas pressures. The pitch angle against the horizontal plane was $\theta = 4.1°$, and L_C = 3.88 m. The neutral pressures, discharge currents and discharge voltages of plasmas were, respectively, (a) p_n = 3.1 mTorr, I_d = 10 A, and V_d = 130 V, (b) p_n = 6.7 mTorr, I_d = 10 A, and V_d = 60 V, and (c) p_n = 1.1 mTorr, I_d = 1 A, and V_d = 190 V. Figures 5 (a - c) show that spiral shape plasmas were generated from the vicinity of the cathode.

Figure 6 shows the 2D distribution of I_{sat} at $\varphi = 90°$. Poloidal cross-section of the cathode was mapped as red squares on the poloidal cross section. The first turn plasma in all p_n was located at radially outer-side edge of the red squares for all the cases.

At p_n = 3.1 mTorr (Fig. 6 (a)), the full widths at half maximum of I_{sat} distribution of the first and second turns were 62 and 77 mm, respectively. Therefore, the broadening ratio of I_{sat} due to plasma transport along the magnetic field line (2 m) was 24%. Further, the second turn plasma was drifted to the lower left. At higher pressure, p_n = 6.7 mTorr (Fig. 6 (b)), the I_{sat} at the peak position of the second turn was very small; I_{sat} distribution was re-plotted in log scale (Fig. 6 (d)). The full widths at half maximum

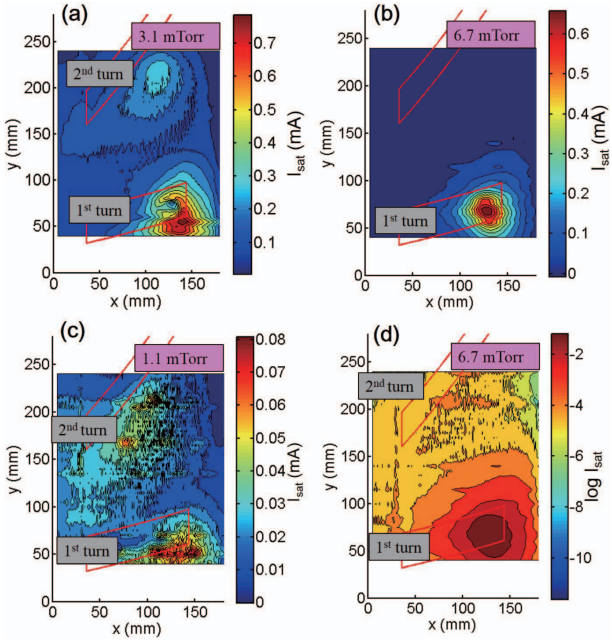

Fig. 6 (a) 2D distribution of ion saturation current at 3.1 mTorr, (b) 6.7 mTorr and (c) 1.1 mTorr. (d) 2D distribution of ion saturation current at 6.7 mTorr in log scale.

of I_{sat} distribution of the first and second turns were 41 and 74 mm, respectively. At a lower pressure, p_n = 1.1 mTorr (Fig. 6 (c)), DC discharge was unstable, leading to the scattered I_{sat} distribution.

3.2 Power dependences of electron temperature and density

We investigated discharge power dependences of T_e and n_e at I_{sat} peak positions in Fig. 6. At p_n = 3.1 mTorr, the plasma parameters were measured in the first and second turns, whereas the parameters was measured only in the second turn at p_n = 6.7 mTorr.

Figure 7 (a) shows the power dependances of T_e. In the first and second turns, T_e increased with the discharge power at p_n = 3.1 mTorr. The T_e decreased to

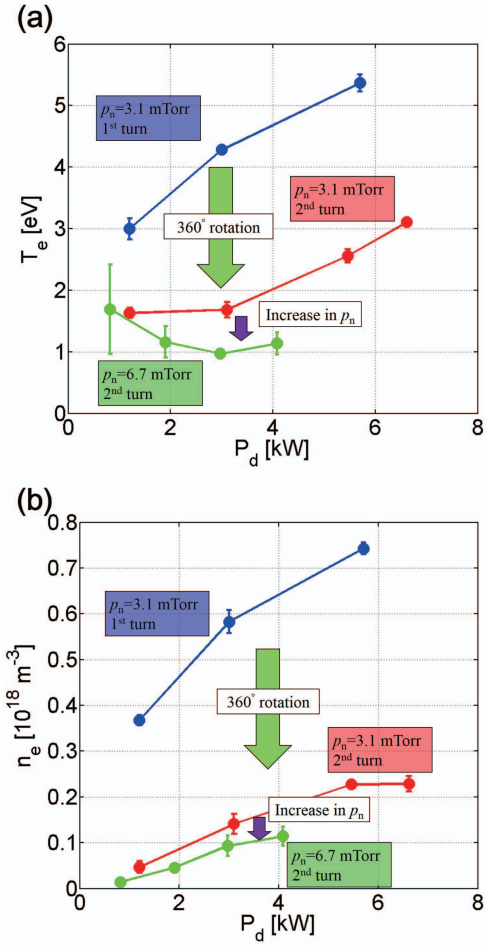

Fig. 7 (a) Power dependences of electron temperature at various situations, and (b) Power dependences of electron density at various situations.

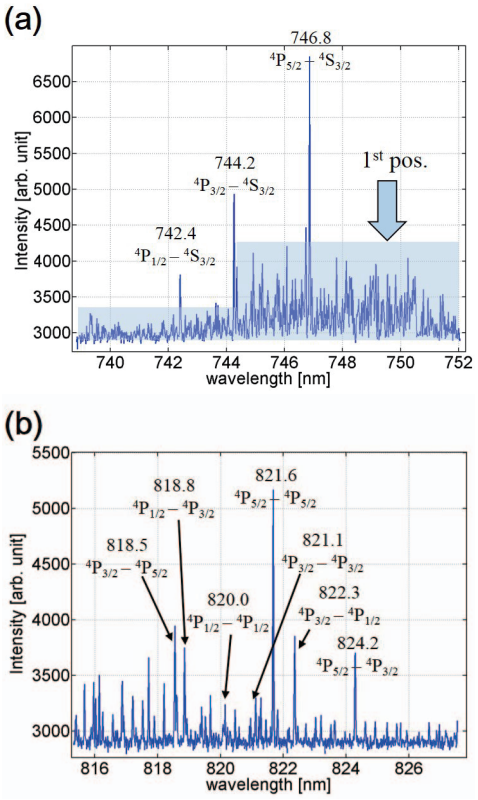

Fig. 8 Spiral shape DC nitrogen discharge emission spectrum around (a) 745 nm, and (b) 821 nm.

approximately half while toroidally rotated from the first to the second turn. At p_n = 6.7 mTorr, T_e in the second turn slightly decreased from T_e at p_n = 3.1 mTorr at $P_d \geq\sim 2$ kW. Figure 7 (b) shows the power dependances of n_e. The first and second turns of n_e at p_n = 3.1 mTorr and second turn of n_e at p_n = 6.7 mTorr increased with the discharge power. The n_e decreased to approximately 70% while toroidally rotated from the first to the second turn. At p_n = 6.7 mTorr, n_e in the second turn slightly decreased from n_e at p_n = 3.1 mTorr.

From the above results, it was found that T_e and n_e strongly decreased along the magnetic field at p_n = 3.1 mTorr. Because the diffusion effect was not so large as described in section 3.1, it was suggested that the second turn plasma at p_n = 3.1 mTorr became recombining plasma. Furthermore, it was suggested that the recombining process was facilitated at p_n = 6.7 mTorr [14].

3.3 Optical emission spectroscopy (OES)

Vaudo *et al.* had performed optical measurement in an ECR nitrogen plasma [15]; first positive series (1PS) emission is prominent around the wavelength of 745 nm. We conducted optical emission spectroscopy in wavelengths around 745 nm and 821 nm.

The discharge condition was as follows: p_n = 3.1 mTorr, I_d = 10 A, and V_d = 110 V. The measurement was conducted at φ = 240°. Figures 8 (a) and (b) show emission spectra at the wavelength around 745 and 821 nm, respectively. Spectra peaks of nitrogen atoms were seen at 742.4 ($^4P_{1/2}-{}^4S_{3/2}$), 744.2 ($^4P_{3/2}-{}^4S_{3/2}$), and 746.8 nm ($^4P_{5/2}-{}^4S_{3/2}$) in Fig. 8 (a). Also, the 1PS was observed in the wavelength range of 739 - 752 nm. Around 845 nm, as was suggested previously [15], many nitrogen atomic emission were identified: 818.5 ($^4P_{3/2}-{}^4P_{5/2}$), 818.8 ($^4P_{1/2}-{}^4P_{3/2}$), 820.0 ($^4P_{1/2}-{}^4P_{1/2}$), 821.1 ($^4P_{3/2}-{}^4P_{3/2}$), 821.6 ($^4P_{5/2}-{}^4P_{5/2}$), 822.3 ($^4P_{3/2}-{}^4P_{1/2}$), and 824.2 nm ($^4P_{5/2}-{}^4P_{3/2}$). It was suggested that both nitrogen atoms and molecules existed in this plasma.

Figure 9 shows discharge power dependences of the ratio of the atomic to molecular emission intensities defined as

$$k_I = \frac{I_{746.8}[\mathrm{N}]}{2\langle I_{1PS}[\mathrm{N_2}]\rangle}, \quad (1)$$

where $I_{746.8}[\mathrm{N}]$ is the emission intensity of 746.8 nm, which is the strongest emission from nitrogen atoms observed, and $\langle I_{1PS}[\mathrm{N_2}]\rangle$ was the averaged 1PS emissions intensity. At p_n = 6.7 mTorr, there was no clear emission when with P_d = 0.89 and 1.6 kW. However, with increasing the discharge power, the emissions were observed at

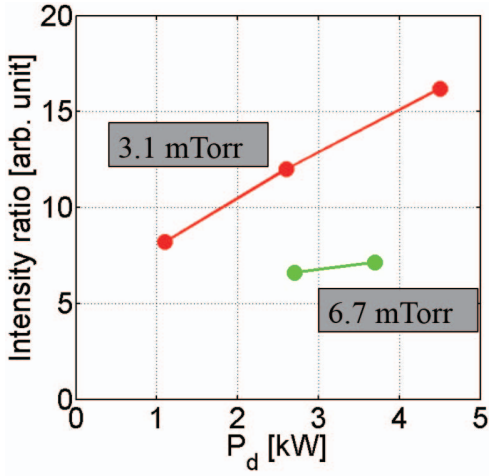

Fig. 9 Discharge power dependences of k_I.

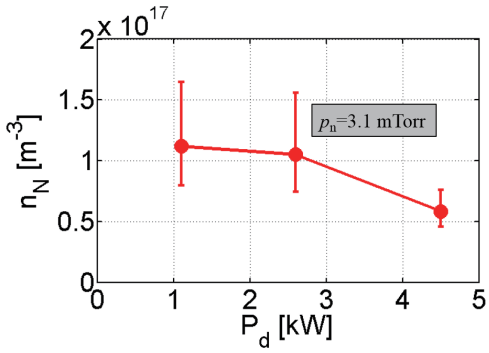

Fig. 10 Discharge power dependences of densities of ground state nitrogen atom.

P_d = 2.7 kW, and k_I increased slightly at P_d = 3.7 kW. At p_n = 3.1 mTorr, with increasing the discharge power to P_d = 4.6 kW from P_d = 1.1 kW, k_I increased and was greater than at p_n = 3.1 mTorr. As will be discussed later, this was probably caused by the variation in T_e.

Since the population distribution was mainly determined by recombination component in recombining plasmas, which is not sensitive to the atomic density, it is difficult to assess the atomic density from the emission intensity. However, here, since the electron temperature could be higher than 2 eV at p_n = 3.1 mTorr, it was likely that the population was mainly determined by the electron impact excitation, though the process to generate atomic nitrogen could be mainly produced by dissociative recombination, as was described previously. Thus, for the first trial, we estimated the atomic nitrogen density with applying coronal equilibrium to the excited states. The densities of $3p\ ^4S_{2/3}$ state nitrogen atom can calculate as

$$\frac{I^*_{746.8}[\mathrm{N}]}{A(3p\ ^4S_{3/2}, 3s\ ^4P_{5/2})} = n(3p\ ^4S_{3/2}), \tag{2}$$

where $I^*_{746.8}$[N] [sr^{-1}nm^{-1}m^{-2}s^{-1}] is the calibrated intensity and $A(3p\ ^4S_{3/2}, 3s\ ^4P_{5/2})$ is the transition probability of deexcitation to $3s\ ^4P_{5/2}$ from $3p\ ^4S_{3/2}$. Assuming that electron impact excitation from the ground state is the dominant production process, the density of ground state $(2p\ ^4S_{3/2})$ nitrogen atom can be calculated using the following relation [16]:

$$n(3p\ ^4S_{3/2}) = \frac{C(2p\ ^4S_{3/2}, 3p\ ^4S_{3/2})\, n_e}{\sum_{<3p\ ^4S_{3/2}} A}\, n(2p\ ^4S_{3/2}), \tag{3}$$

where $\sum_{<3p\ ^4S_{3/2}} A$ is the sum of the all transition probability of deexcitation from $3p\ ^4S_{3/2}$. The rate coefficient C can be obtained in [17]. We could not measure T_e and n_e at the same position as the OES; we interpolated the value from the electrostatic probe measurement performed at 150 and 210 degrees upstream and downstream from the OES position, respectively.

Figure 10 shows the discharge power dependences of densities of ground state nitrogen atom. The error of the nitrogen atom density (n_N) was assessed here that interpolated T_e and n_e has errors of ±20% in the interpolated angles. The n_N was approximately 1×10^{17} m^{-3}.

It should be noted that the actinometry measurement method which uses emission intensity of Ar atom and collisional-radiative model is well known assessing the accurate density [18].

4. Summary

We have proposed a new method to generate high density nitrogen atoms based on dissociative recombination of molecular nitrogen ions. The usefulness of this method was experimentally verified in the toroidal plasma device, NAGDIS-T. Generation of high density nitrogen plasma along the spiral shape magnetic field was confirmed by 2D distribution of I_{sat} measurements. The electron temperature T_e and density n_e strongly decreased while the plasma toroidally being rotated from the first to second turn and also increased in neutral pressure p_n. The optical emission spectroscopy suggested that both nitrogen atoms and molecules existed in the plasma. The ratio of the atomic to molecular emission intensities increased with the discharge power. The atomic nitrogen density n_N estimated with applying coronal equilibrium was ~10^{17}m^{-3}.

Acknowledgments

This research was supported by Grant-in-Aid for Challenging Exploratory Research (17K18768) from the Japan Society for the Promotion of Science (JSPS). This research was also supported by a grant from the Hibi Science Foundation and the NINS program of Promoting Research by Networking among Institutions (01411702). The authors are deeply grateful to Mr. M. Takagi for technical support.

[1] T. Takase, Tetsu-to-hagane **66**, 9, 1423 (1980).
[2] M. Hudis, J. Appl. Phys. **44**, 1489 (1973).
[3] J.M. Hendrie, J. Chem. Phys. **22**, 1503 (1954).
[4] S. Tada *et al.*, J. Appl. Phys. **88**, 1756 (2000).
[5] H. Shoyama *et al.*, J. Vac. Sci. Technol. **24**, 1999 (2006).
[6] St. Halas *et al.*, Int. J. Mass Spectram. Ion Phys. **10**, 157 (1972).
[7] J.R. Peterson *et al.*, J. Chem. Phys. **108**, 1978 (1998).
[8] H. Tahara, *et al.*, IEEE Trans. Plasma Sci. **26**, 1307 (1998).
[9] Q.S. Yu *et al.*, Plasma Chem. Plasma Proc. **18**, 461 (1998).
[10] L. Robin *et al.*, Phys. Plasmas **1**, 444 (1994).
[11] H. Akatsuka *et al.*, IEEE Trans. Plasma Sci. **42**, 3691 (2014).
[12] R. Ichiki *et al.*, Mater. Lett. **71**, 134 (2012).
[13] K. Yada *et al.*, J. Nucl. Mater. **390-391**, 290 (2009).
[14] N. Ohno, Plasma Phys. Control. Fusion **59**, 3, 034007 (2017).
[15] R.P. Vaudo *et al.*, J. Vac. Sci. Technol. B: **12**, 1232 (1994).
[16] M. Goto *et al.*, J. Plasma Fusion Res. **79**, 12, 1287 (2003).
[17] R.M. Frost *et al.*, J. Appl. Phys. **84**, 6 (1998).
[18] Y. Ichikawa *et al.*, Jpn. J. Appl. Phys. **49**, 106101 (2010).